Title: Tertiary lymphoid structure signatures are associated with immune checkpoint inhibitor related acute interstitial nephritis

Authors: Shailbala Singh[1], James P. Long[2], Amanda Tchakarov[3], Yanlan Dong[4], Cassian Yee[1,5*], Jamie S. Lin[4*]

[1]Department of Melanoma Medical Oncology, The University of Texas MD Anderson Cancer Center, Houston, TX, USA

[2]Department of Biostatistics, Division of Basic Sciences, The University of Texas MD Anderson Cancer Center, Houston, TX, USA

[3]Department of Pathology and Laboratory Medicine, University of Texas Health Science Center McGovern Medical School, Houston, TX, USA

[4]Section of Nephrology, Division of Internal Medicine, The University of Texas MD Anderson Cancer Center, Houston, TX, USA

[5]Department of Immunology, The University of Texas MD Anderson Cancer Center, Houston, TX, USA

Corresponding Authors:

Cassian Yee, M.D., Professor, Department of Melanoma Medical Oncology, The University of Texas MD Anderson Cancer Center; email: cyee@mdanderson.org; phone: (713) 563-3750

Jamie S. Lin, M.D., Assistant Professor, Section of Nephrology, Division of Internal Medicine, The University of Texas MD Anderson Cancer Center, email: jlin8@mdanderson.org; phone: (713) 745-9331

Conflict of Interest: The authors have declared that no conflict of interest exists.

ABSTRACT

Tertiary lymphoid structures (TLSs) are associated with anti-tumor response following immune checkpoint inhibitor (ICI) therapy, but a commensurate observation of TLS is absent for immune related adverse events (irAEs) i.e. acute interstitial nephritis (AIN). We hypothesized that TLS-associated inflammatory gene signatures are present in AIN and performed NanoString-based gene expression and multiplex 12-chemokine profiling on paired kidney tissue, urine and plasma specimens of 36 participants who developed acute kidney injury (AKI) on ICI therapy: AIN (18), acute tubular necrosis (9), or HTN nephrosclerosis (9). Increased T and B cell scores, a Th1-$CD8^+$ T cell axis accompanied by interferon-γ and TNF superfamily signatures were detected in the ICI-AIN group. TLS signatures were significantly increased in AIN cases and supported by histopathological identification. Furthermore, urinary TLS signature scores correlated with ICI-AIN diagnosis but not paired plasma. Urinary CXCL9 correlated best to tissue *CXCL9* expression (rho 0.75, $p < 0.001$) and the ability to discriminate AIN vs. non-AIN (AUC 0.781, p-value 0.003). For the first time, we report the presence of TLS signatures in irAEs, define distinctive immune signatures, identify chemokine markers distinguishing ICI-AIN from common AKI etiologies and demonstrate that urine chemokine markers may be used as a surrogate for ICI-AIN diagnoses.

INTRODUCTION

Tertiary lymphoid structures (TLSs) are ectopic organized aggregates of immune cells that develop in non-lymphoid tissues at the sites of chronic inflammation (1). Similar to secondary lymphoid organs (SLO), mature TLSs are characterized by a T cell zone interspersed with dendritic cells (DCs) and a germinal center with proliferating B cells. Stimulation of immune cell interactions by pro-inflammatory cytokines leads to the development of TLSs and the generation of autoreactive T and B cells and resultant local production of autoantibodies (2). Whether appearance of TLS is desirable or not is dependent on the pathological context in which they exist. In autoimmune diseases, TLS formation is associated with disease persistence and worsened clinical outcomes; while in solid tumors, TLS formation is associated with anti-tumor response and improved clinical outcomes (2). In fact, the efficacy of immune checkpoint blockade has been correlated with the detection of TLS in tumor by immunohistochemical (IHC) analysis or by TLS gene signature(s) in patients with melanoma, breast cancer, colorectal cancer, non-small cell lung cancer and pancreatic cancer where TLS has been suggested to be a reliable, predictive biomarker of immune checkpoint inhibitor (ICI) therapy response (3).

ICI therapy can be a highly effective cancer treatment option but increasing T-cell activity can also increase T cell autoreactivity leading to the development of immune related adverse events (irAEs). Over 60% of patients treated with immune checkpoint blockade will develop at least one irAE (4, 5). Since the development of irAEs is associated with increased immune activity, studies among more common irAEs, such as dermatitis, colitis and various endocrinopathies, are linked with increased ICI efficacy. Less is known, however, in patient outcomes for uncommon irAEs such as renal irAEs, which usually manifest as acute interstitial nephritis (AIN) (6). Although 15-20% of patients on immune checkpoint blockade will develop acute kidney injury (AKI), only 2-5% of cases will be AIN (6-8). Timely and accurate diagnosis of AIN is complicated due to the lack of non-invasive diagnostic tests; as such, kidney biopsy remains the gold standard. In patients with cancer, a kidney biopsy may not always be feasible and when performed may carry a significant risk of morbidity such as major bleeding complications in 1.6-5% of cases;

consequently, steroid therapy is often initiated empirically for presumed ICI-AIN (9-13). Difficulties in diagnosing AIN, the low frequency of ICI-AIN occurrence, and delays in AKI management contribute to the development of permanent functional kidney loss in over 50% of ICI-AIN patients despite glucocorticoid therapy (14). A greater understanding of the pathophysiology of ICI-AIN will improve our ability to accurately diagnose AIN and enable prompt implementation of therapeutic strategies.

To address this knowledge gap, we asked whether differential expression of genes could be uncovered in kidney tissue biopsies of patients who developed AKI on ICI therapy that distinguishes AIN from other kidney pathologies such as acute tubular necrosis (ATN) or hypertensive (HTN) nephrosclerosis. We report significant increases in genes associated with pro-inflammatory cytokines and immune cells in the ICI-AIN group compared to the ATN or HTN nephrosclerosis groups which led us to inquire if TLS signatures could be detected. Finally, we asked whether these kidney biopsy results correlated with paired urine and plasma specimens providing a less invasive means of detecting ICI-AIN in patients receiving immune checkpoint therapy. This study is, to our knowledge, the first to demonstrate the presence of distinguishing TLS features in ICI-AIN and in fact, any ICI-associated toxicity, that is detectable in both tissue and urine.

RESULTS

Cohort characteristics and kidney injury assignment

We enrolled 36 patients who had received ICI therapy and underwent a clinically indicated kidney biopsy for AKI evaluation at The University of Texas MD Anderson Cancer Center (Figure 1). Relevant clinical and pathological characteristics are presented in Table 1. The participants were grouped according to their major pathological biopsy diagnosis of AIN, ATN or HTN nephrosclerosis and comparisons were made for different demographic and pathological parameters. A greater proportion of patients were males in the ICI-AIN group. Only two participants received anti-PD-L1 therapy. While baseline levels of creatinine were higher in the HTN group (Cr 1.30 mg/dl) compared to both AIN (1.00 mg/dl) and ATN (0.90 mg/dl) groups, average peak serum creatinine was identified to be higher in ICI-AIN compared to ATN and HTN. Ten out of the 18 ICI-AIN cases had stage 3 AKI (4 stage 2, and 4 stage 1) by KDIGO criteria (15). In the ATN group, each AKI stage was equally represented (3 stage 1, 3 stage 2 and 3 stage 3). For the HTN group, almost all patients were AKI stage 1 (3 stage 1, 0 stage 2, 1 stage 3). Percent of inflammation in the renal cortex was significantly higher in ICI-AIN compared to ATN and HTN groups (16). Median time from first ICI infusion to AKI for AIN was 145 days, 67 days ATN group and 197 days in the HTN group. Almost all ICI-AIN patients received corticosteroid therapy with 7 patients achieving complete renal recovery, 8 partial renal recovery and 3 with no renal recovery. In the ATN group, 2 patients achieved complete renal recovery and 7 had partial renal recovery. For the HTN group, 5 of the 9 patients had complete renal recovery while 3 had partial and 1 had no renal recovery. Only 2 of the ICI-AIN patients were re-challenged on ICI therapy while 6 of the 9 ATN and all HTN group participants resumed ICI therapy.

Renal pathology and cellular characterization of immune cell infiltrates

The clinical diagnosis of AKI was made by histological examination of the biopsied kidney tissue by the renal pathologist. Representative images are shown in Figure 2. Histopathological analysis of the kidney biopsy showed that AIN was characterized by dense lymphocytic infiltrates along with varying numbers

of neutrophils, plasma cells and eosinophils. Often lymphocytic tubulitis was present, which in some cases was severe with associated tubular basement membrane disruption. By comparison, cases of ATN showed tubular epithelial injury that manifested as ectatic, flattened epithelium and loss of brush borders. Interstitial inflammation associated with ATN was minimal to mild consisting predominantly of lymphocytes and plasma cells and tubulitis was minimal, if present, but was typically absent. Cases of HTN nephrosclerosis showed absent to minimal interstitial infiltration by lymphocytes and plasma cells and tubulitis was not present.

Identification of differentially expressed genes and infiltrating immune cells in AIN

AIN and ATN are the most frequently reported kidney pathologies from biopsied cancer patients on ICI therapy. Although both are acute conditions of kidney injury with similar clinical presentation, only AIN can be treated with glucocorticoids and ATN is generally considered to be a toxic ischemic injury without any specific therapy. This divergent response to anti-inflammatory therapy combined with distinct lymphocyte infiltration patterns observed in renal pathology strongly suggests a difference in the immune gene expression profile in AIN and ATN. To identify the genes that are differentially expressed in these two pathologies, we performed a comprehensive gene expression analysis using NanoString nCounter PanCancer Immune Profiling Panel. Out of 770 genes evaluated, in AIN vs ATN, a total of 23 differentially expressed genes (DEGs) with a fold change ± 4 (p-Adj < 0.01) was detected. These genes were upregulated in AIN compared to ATN. Among the DEGs eight of the top ten most differentially expressed genes were inflammatory chemokines and immune associated genes (*CCL18, CXCL11, CXCL10, CXCL9, CXCL8, CXCL7, TREM1*) and *(SLAMF1)* a gene associated with activated T and B lymphocytes (Figure 3A and Table 2). Between AIN and HTN, a total of 159 differentially expressed genes with a fold change ± 4 were detected (p-Adj < 0.01). Similar to AIN vs ATN, the top ten DEGs were inflammatory chemokines (*CCL18, CCR7, CXCL10, LTF, CXCL9, CXCL6, CCL13*) and genes associated with AKI (*SAA1, LCN2, C3*) (Figure 3A and Table 3). In contrast, comparison of gene expression profile of ATN and HTN groups revealed differentially expressed genes that are different from the AIN group (Supplemental Figure 1) suggesting an unrelated etiology for ATN.

To determine if the elevated chemokine profile was associated with increased immune cell infiltration in the kidney tissue, we used immune cell gene signatures to compare cell scores among AIN, ATN and HTN groups. These scores are indicative of the relative abundance of cells in the tissue (17, 18). Consistent with the pathology findings, AIN cases had significantly higher immune cell scores for T and B lymphocytes, macrophages, neutrophils and dendritic cells compared to both the ATN and HTN group (Figure 3B). We did not detect a difference in the natural killer (NK) cell score among the three groups (Figure 3B).

Deconvolution of T cell composition and their function

Different T cell subtypes, namely $CD8^+$ T cells and Th17, have been identified for commonly occurring irAEs such as colitis and rheumatoid arthritis (19-22). However, the specific immune cell subsets and mechanism of pathogenesis associated with ICI-AIN are underexplored. We used NanoString analysis to deconvolute immune cell gene expressions to identify and determine the abundance of T cell subsets infiltrating the kidneys. Our analysis showed an increase in Th1 cell score in the ICI-AIN group compared to HTN group but no differences in Th2 or Th17 cell scores amongst the three groups (Figure 4A). A statistically significant increase in cytotoxic $CD8^+$ T cell score was also detected in the AIN group compared to the ATN and HTN groups (Figure 4C). No difference in the abundance of infiltrating T regulatory (T reg) cells was detected in the three groups (Figure 4B).

Since interferon (IFN)-γ inducible chemokines *CXCL9, -10* and *-11* were observed to be differentially expressed in AIN vs ATN and an increase in the Th1 cell subset score was also observed, we interrogated the three groups for genes associated with an IFN-γ signature. Our data revealed a significant upregulation in the IFN-γ signature in the AIN group (compared to ATN and HTN groups) suggesting that IFN-γ is the likely mediator of the Th1 immune response in ICI-AIN (Figure 4D).

The TNF superfamily (TNFSF) plays a pivotal role in the modulation of inflammation and autoimmunity and elevated levels of TNF-α have been reported in several irAEs. Inhibition of the TNF axis has been successful in treating inflammatory conditions such as ICI-mediated nephritis, colitis and arthritis (23-25). Several TNFSF members are also associated with TLS development (26). To evaluate for the possible involvement of TNF modulation in ICI-AIN we investigated the TNFSF gene expression signature. Our results showed significant upregulation of the TNFSF signature and *TNF* expression (Figure 4E) in the ICI-AIN group compared to ATN and HTN groups (Table 4 and Table 5). Studies have shown that both Th1 and Th17 cells can secrete TNF-α. Unlike several other irAEs such as colitis and rheumatoid arthritis that are associated with a Th17 profile, our observations, based on cell subtype score, IFN-γ and TNFSF expression profile, suggest that ICI-AIN is Th1 mediated.

Tertiary Lymphoid Structure (TLS) signatures are observed in ICI-AIN

ICIs can induce pro-inflammatory cytokines and TNF superfamily members promote localized interactions between inflammatory immune cells and resident stromal cells leading to the formation of TLS in tumor (2). ICI-triggered TLS development in tumor has been associated with clinical response in various cancer types; however, irAEs which are unique ICI side effects that resemble autoimmune responses have not been evaluated for the presence of TLS. Based on the histologic and gene expression findings above, we investigated whether TLS development is associated with ICI-AIN. We used an established, well-validated 12-chemokine TLS gene signature (*CCL2, CCL3, CCL4, CCL5, CCL8, CCL18, CCL19, CCL21, CXCL9, CXCL10, CXCL11*, *CXCL13*) that is correlated with improved survival among patients with colorectal cancer, melanoma and breast cancer (27-29). Gene expression analysis of kidney biopsies demonstrated a statistically significant upregulation in the TLS signature in the AIN group compared to the ATN and HTN groups ($p<0.05$) (Figure 5A). Amongst the 12 chemokines, *CXCL13, CCL19 and CCl21*, in particular, have been shown to regulate lymphocyte homing and lymphoid neogenesis where ectopically expressed *CXCL13* is sufficient to induce lymphoid neogenesis (30-32). Expression levels of *CXCL13* and *CCL19* were significantly increased in ICI-AIN compared to ATN or

HTN groups while *CCL21* in ICI-AIN was significantly increased when compared to HTN group (Figure 5B and 5E).

To further validate the TLS signature found in ICI-AIN, we find a strong association of the ICI-AIN gene signature with TLS signatures for melanoma (*CCL19, CCL21, CXCL13, CCR7, SELL, LAMP3, CXCR4, CD86, BCL6*) and urothelial cancer (*CD79A, MS4A1, LAMP3, POU2AF1*), where several B cell genes associated with improved antigen presentation, and increased cytokine-mediated signaling were found to be significantly enhanced (33, 34). A significant upregulation in the expression of genes associated with melanoma TLS and urothelial TLS signatures was observed in the AIN group compared to the ATN and HTN groups (Figure 5A, $p < 0.01$).

The TLS signature for breast cancer also includes genes associated with T follicular helper (Tfh) cells which play a major role in the humoral immune response by facilitating B-cell activation, function and differentiation to memory B cells and plasmablasts leading to germinal center formation and mature TLS. Since we observed an increased B cell score in our earlier analysis, we investigated the TLS signature in breast carcinoma (*CD200, PDCD1, CXCL13, CXCL9, CD38, ICOS, IFNG, CXCL13* alone) that includes Tfh (*CD200, PDCD1* plus *CXCL13*) and Th1 genes (*CD38, CXCL9, INFG*) in ICI-AIN. In fact, the TLS signature that predicts breast cancer survival was found to be significantly elevated in ICI-AIN but not in the ATN or HTN groups (Figure 5A, $p < 0.01$) supporting the presence of TLS development in ICI-AIN (35).

To evaluate for the morphologic presence of TLS in the ICI-AIN group, microscopic examination of hematoxylin and eosin (H&E) stained sections of the kidney biopsy was performed by a renal pathologist blinded to the biopsy diagnosis (1). TLS was defined as organized, dense lymphoid aggregates composed of a large cluster of lymphocytes (≥ 50) with expansion of the involved interstitium. Histological assessment of the ICI-AIN biopsies revealed tertiary lymphoid-like structures and the presence of CD20

positive B cells adjacent to a CD3 positive T cell zone (Figure 5C) (1, 36-38). To account for the variations in the amount of renal cortex obtained on kidney biopsy, we calculated the abundance or density of TLS per case. TLS density was determined by dividing the total number of tertiary lymphoid-like structures by the total biopsied kidney cortex area [mm^2]. A significantly greater TLS density was observed in the ICI-AIN group compared to HTN (Figure 5D). Supervised clustering of chemokines revealed an association of almost all chemokines with TLS formation in the AIN group. Based on immune cell gene scores, in cases of ICI-AIN an association was also observed with infiltration of DCs, T cells, macrophages, B cells and neutrophils (Figure 5E). Clustering of B cell genes expressed in the ICI-AIN cohort suggests that B cells (*REL, LTB, CD20, CXCR5, PAX5, IRF8*) were activated and differentiating into plasmablasts (*CD62L, IRF4*) and progressing towards organization of germinal centers (*VCAM1, ITGA2B, TNFRSF17/BCMA*, Figure 5E) (39, 40).

Elevated levels of urinary chemokines associated TLS in urine from ICI-AIN patients

Kidney biopsies, especially in cancer patients, poses an increased risk of bleeding, and thus is not always a feasible option (9-12). With the incidence of post-renal biopsy hematomas ranging up to 11%, a non-invasive approach that uses urine or plasma sampling represents an attractive solution for facilitating detection and monitoring of patients on ICI therapy (13). Based on the transcriptomic profiling data, we developed a customized multiplex panel of 12 chemokines associated with the TLS signature and measured the levels of the selected chemokines in paired urine and plasma specimens. Using Luminex based assay, we were unable to detect a difference in plasma TLS scores among the AIN, ATN or HTN groups (Figure 6A). However, in urine an overall greater 12 chemokine TLS score was observed with ICI-AIN compared to the HTN group (Figure 6A). To test the utility of these various methods, we sought to determine whether ICI-AIN vs non-AIN (ATN or HTN) can be predicted by either tissue TLS gene expression score, TLS density or urine or plasma TLS scores. Our analysis showed that the tissue TLS gene expression signature can perfectly separate AIN from non-AIN (AUC 1.00 $p < 0.001$) followed by TLS density (0.841, $p < 0.001$) and urine TLS score (0.735, $p = 0.016$, Table 6). Analysis comparing TLS gene expression in tissue to urine TLS score confirmed a greater correlation ($R = 0.64$, $p = 0.0017$)

compared to tissue vs plasma TLS score ($R = 0.35$, $p = 0.15$) which failed to significantly correlate with the TLS gene expression in tissue (Figure 6B).

We then used the 12 chemokine TLS signature shown to be associated with improved clinical outcomes in melanoma, breast and colorectal carcinoma to evaluate the correlation of the individual urinary chemokines to the overall tissue TLS gene signature (28-30). Analysis comparing the individual urine chemokine vs tissue TLS gene signature or individual tissue chemokine gene expression vs urine chemokine level determined a higher correlation in the expression of *CXCL9, CXCL10* and *CCL19* (Table 7 and Table 8) between tissue and urine. Taken together, the close alignment with tissue levels suggests that urine may be well-suited for non-invasive diagnosis and monitoring of acute kidney injury, and in fact superior to plasma (Figure 6B). CXCL9 and CXCL10 in urine demonstrated a greater correlation with kidney tissue samples ($R > 0.6$, $p < 0.005$) and strong ability to discriminate AIN from ATN or HTN (AUC > 0.75, $p < 0.005$) suggesting the utility of this chemokine signature in the urine for diagnosing AIN without an invasive biopsy (Figure 6C and Table 9). Logistic regression was used to determine if several chemokines combined in a single score could improve this discrimination ability. These models achieved marginal improvement over individual chemokines (AUC of 0.82 for logistic regression combination rule vs AUC of 0.80 for CXCL10 alone) which were not statistically significant. This is likely due to the presence of redundant information in the chemokines (CXCL9 and CXCL10 are highly correlated) and a small sample size. These data and analysis show that while gene expression profile of kidney tissue is a superior approach, CXCL9 and CXCL10 expression in urine can be used as biomarkers for diagnosis of AIN.

DISCUSSION

In this study we sought to understand if specific gene signatures could be identified in biopsied cases of ICI-associated AKI caused by AIN compared to ATN or HTN nephrosclerosis. Here we report significantly increased accumulation of immune cells, upregulation of pro-inflammatory cytokines *CXCL9* and *CXCL10*, and IFN-γ and TNFSF signatures in cases of ICI-AIN compared to those with ATN or HTN nephrosclerosis. For the first time, TLS gene signatures have been observed in renal irAEs specifically, ICI-AIN, by histologic examination, and present in paired *urine* specimens by protein ELISA, providing an opportunity for non-invasive monitoring of ICI-AIN. This study represents the first demonstration of TLS signatures in ICI-associated nephritis and, in fact, any irAE-affected tissue.

AKI is a common manifestation in patients with cancer receiving ICI therapy, etiologies include ischemic nephrotoxic tubular injury which can be manifested by ATN lesions, hemodynamic fluctuations in patients with underlying HTN nephrosclerosis, or AIN (41, 42). Since patients with ICI-AIN respond to glucocorticoid therapy unlike ATN or HTN, we investigated the underlying mechanisms leading to the development of this condition (43). Our gene expression profile analysis confirmed the morphologic characteristics seen microscopically on kidney biopsy which suggests that ICI-AIN is distinct from both ATN and HTN nephrosclerosis. AIN is characterized by lymphocytic infiltration of the renal cortex and by gene expression analysis, ICI-AIN displayed an upregulation in genes associated with chemokine signaling and significant increases in immune cell scores compared to ATN and HTN nephrosclerosis.

T helper cells have also been shown to be associated with autoimmune diseases and irAEs but a definitive role in ICI-AIN has not been previously investigated. Differential upregulation of Th1 associated genes but not Th2 or Th17 associated genes were detected in ICI-AIN (Figure 3E). In other irAEs (e.g. ICI-associated arthritis and colitis), a Th17 signature was reported (19-22). We did not detect a similar signature with Th17 enrichment in ICI-AIN suggesting that the pathogenic mechanisms amongst irAEs may either be distinct or the plasticity of Th17 to Th1 cells may be involved (19, 44). In glomerulonephritis,

another immune mediated kidney lesion, a transition from Th17 dominance at early stages to Th1 dominance at later stages of disease development has been reported (44, 45). Since differentiation of T cells to Th1 cells is initiated by the presence of IFN-γ and our analysis showed increased Th1 genes, we investigated whether an IFN-γ signature could be detected. As postulated, the IFN-γ score for ICI-AIN was significantly increased compared to both the ATN and HTN groups (Figure 4D). Additionally, IFN-γ –induced chemokines: *CXCL9*, *CXCL10*, *CXCL11*, were the most differentially upregulated genes in ICI-AIN compared to ATN (Figure 3A). CXCL9, -10 and -11 are secreted by monocytes, endothelial cells, fibroblasts and cancer cells and with its ligand CXCR3 form a paracrine axis that regulates immune cell response by modulating migration, differentiation and activation (46). Th1 cells also secrete TNF-α and in chronic inflammatory conditions such as psoriasis and atherosclerosis as well as cancer, both IFN-γ and TNF-α can synergistically increase the expression of CXCL9, CXCL10 and CXCL11, hence we also confirmed a TNFSF signature (46, 47).

Of particular interest in this study is the identification of TLS signatures as a distinguishing feature of ICI-AIN. TLS have been identified within a wide range of human cancers and at all stages of disease (48-51). In primary and metastatic lesions, TLS have the same characteristics as in their primary sites but TLS in irAEs have not previously been identified. While further histological confirmation of TLS would be desirable, we believe that the results presented, both by histopathological analysis and gene expression profiles are highly suggestive of TLS and would be confirmatory for a TLS signature in cases of irAEs (32, 37, 38). Increased levels of CXCL 9, -10 and -11 have been strongly associated with irAEs and are a major focus in antitumor immunity where they have been implicated in the formation of TLS (28, 52, 53). Since CXCL 9 and 10 were amongst the top differentially upregulated genes and an increase in IFN-γ and TNFSF along with an abundance of T and B cells were detected in our ICI-AIN cohort, we hypothesized that TLS signatures may be present in ICI-AIN. We used a well-established 12 chemokine TLS signature to confirm an increase in ICI-AIN vs non-AIN cases and further validated our results with three additional TLS gene expression signatures (34, 35, 48). Gene analysis for cellular components of

TLS showed expression of B cells (*REL, LTB, CD20, CXCR5, BCL6*) and plasmablast associated genes (*IRF4, CD62L*) in the ICI-AIN cohort which likely reflects the TLS stage in which biopsies were obtained. Since TLS are also present in autoimmune conditions such as lupus nephritis and renal allograft rejection and is associated with end organ damage (40, 54-56), we suspect that mature TLS with GC if observed in ICI-AIN would be functional and involved in active kidney disease.

Since the development of TLS and more frequently occurring irAEs such as dermatitis, colitis and various endocrinopathies have been associated with increased ICI anti-tumor efficacy, we investigated whether there was any difference in overall survival or progression free survival in AIN, ATN or HTN group and found no statistical difference (Supplemental Figure 2). Diagnosis of the more common irAEs are readily made by the presentation of clinical symptoms and specific laboratory tests. These irAEs can be quickly treated enabling patients to continue ICI therapy without significant delays; however, the diagnosis of ICI-AIN is complicated and re-challenge of ICI therapy is infrequent (only 2 patients with ICI-AIN were re-challenged) (57). We postulate whether discontinuation of ICI therapy in the AIN group curtailed the anti-tumor benefits that would be more apparent with ICI therapy continuation.

While corticosteroids are first line therapy in ICI-AIN treatment, not all patients respond to steroid therapy and some will experience ICI-AIN relapse after therapy completion. We have previously shown that short-term use of infliximab, a monoclonal antibody blocking TNF-α, is able to induce durable renal response in ICI-AIN patients who had failed first-line glucocorticoid therapy without compromising overall survival (25). Our data confirmed increased *TNF* expression in ICI-AIN and the top TNF superfamily members differentially expressed in ICI-AIN are not only associated with T and B cell activation, proliferation and differentiation (*TNFRSF4*/*OX40* and *TNFRSF13C/BAFFR*), but have fundamental roles in TLS formation (*LTB, TNFSF14/LIGHT)* and are associated with maintaining the survival of plasma cells and autoantibody secretion (*BCMA*/*TNFRSF17)* (58-60). These data suggest that TNF superfamily members are involved in the pathogenesis of ICI-AIN and TLS, and likely, the clinical response observed is a result

of targeting TNF-α for the treatment of ICI-AIN. Furthermore, in non-ICI associated AIN, increased urinary TNF levels have been reported (60).

The nonlymphoid and tissue specific location of TLS makes it challenging to diagnose or investigate their formation through systemic serum chemokine assays and most diagnoses rely on the classical approach of histopathological examination of biopsy. Further, dilution of locally secreted chemokines in systemic circulation will limit the ability to detect low levels of chemokines that are relevant for differential diagnosis. Since urine can closely reflect the local immune landscape of the kidney, urinalysis is a commonly used noninvasive approach for differential diagnosis and monitoring of several acute and chronic renal diseases (61-64). Our analysis of the 12 chemokine TLS signature between kidney tissue vs urine and kidney tissue vs blood showed that urine had a closer correlation to tissue than plasma suggesting that the differential diagnosis of AIN from ATN and HTN nephrosclerosis is possible using urine and will be superior to a plasma source. Similar differences in the ability to detect AIN associated cytokines in urine and not blood has recently been reported (60). In the current study the magnitude of the urine TLS score is greater for AIN compared to ATN or HTN; however, the small sample size of patients could explain the lack of statistical significance between the different groups. We postulated that individual urine chemokines may have a stronger association to the overall TLS signature score and identified CXCL9 as the best individual marker correlating with the overall tissue TLS signature and individual gene expression. Out of the 12 individual chemokines, urinary CXCL9 and 10 exhibited the greatest ability to discriminate AIN vs non-AIN.

Our study had several strengths including the use of three different approaches; histopathology, gene expression profile and multiplex chemokine assay, to differentiate ICI-AIN from ATN and HTN nephrosclerosis. We validated our findings by using alternatively defined gene expression signatures and histopathological adjudication by the pathologist blinded to the diagnosis. The retrospective nature of this study is the primary limitation of the study resulting in a relatively small number of cases in the different

cohorts and inability to further subclass by ICI therapy. Another limitation is the limited amount of residual biopsy material which only permitted analysis of 770 genes using NanoString nCounter platform. Despite these limitations, this work is the first to demonstrate the presence of TLS signatures in irAEs and to identify several distinct immune signatures in ICI-AIN compared to ATN and HTN nephrosclerosis associated AKI in patients receiving ICI therapy. This work is also the first to demonstrate that urine may be a better biological fluid for non-invasive diagnosis and monitoring of acute kidney injury. Since the development or detection of TLS appears to be of paramount importance in positive anti-tumor response, additional investigation with larger numbers of cases will be necessary to determine if TLS development or characteristics of TLS in normal tissue (i.e. irAE organ sites) correlates with anti-tumor immune activity, and to investigate chemokine protein expression at tissue level to determine whether these inflammatory chemokines localize to TLS. Additionally, longitudinal analysis of urine specimens and clinical information would help clarify the utility of CXCL9 as a marker to monitor treatment response. With greater application of ICI therapy for treating patients with a broader range of cancer types, understanding the significance of TLS in irAEs is imperative for balancing the need for continued anti-tumor therapy with optimal clinical irAE management.

In conclusion, our study is the first to demonstrate the presence of several TLS signatures in renal irAEs and to define gene expression and chemokine signatures associated with ICI-AIN. Together these findings represent an important advancement in our understanding of irAE pathogenesis. This study also highlights the need to further investigate the clinical significance of TLS in irAEs for optimal patient outcomes.

METHODS

Patients and collection of tissue samples

All patients provided informed consents for collection of peripheral blood and urine and access to residual formalin fixed paraffin embedded (FFPE) kidney biopsy tissue. We enrolled adult participants (over the age of 18) with cancer receiving ICI therapy who were scheduled to undergo a clinically indicated kidney biopsy. All patients received either programmed cell death protein 1 (PD-1) inhibitors: pembrolizumab or nivolumab, programmed death-ligand 1 (PD-L1) inhibitors: durvalumab, atezolizumab, or avelumab or combined PD-1 with cytotoxic T-lymphocyte-associated protein 4 (CTLA-4) inhibitors: ipilimumab or tremelimumab. Cases were grouped according to their pathological diagnosis and clinical history. This is a retrospective investigation that included a total of 36 cases (Figure 1).

Data on patient demographics, comorbidities, medications, cancer type and stage, and laboratory test results were obtained through the electronic health record system. We defined AKI using Kidney Disease: Improving Global Outcomes (KDIGO) classification guidelines (15). Progression-free survival (PFS) was defined as the time interval from ICI initiation to progression or death, whichever occurred first. Overall survival (OS) was defined as the time interval from ICI initiation to death. For events that had not occurred by the time of data analysis, times were censored at the last contact at which the patient was known to be alive or free of progression.

Histochemistry

FFPE kidney biopsy tissue (4 μm sections) were deparaffinized in xylene and rehydrated through a graded alcohol series. Sections were then stained with Mayer's Hematoxylin, rinsed with water and counterstained with Eosin. For CD3 (Agilent, GA503) and CD20 (Agilent, GA604) staining, following deparaffinization and rehydration, slides were blocked with peroxidase and incubated with primary antibody followed by DAB enhancer and hematoxylin counterstain. Slides were then dehydrated through a graded alcohol series, cleared with xylene and mounted with coverslips.

Histological scoring

Pathological scoring for TLS for all cases were blinded and reviewed by a renal pathologist (16). TLS were quantified using Hematoxylin and Eosin (H&E) immunohistochemistry staining. Organized, dense lymphocytic aggregates (≥50 lymphocytes) and expansion of involved interstitium were identified as tertiary lymphoid like structures having histological features analogous to that of lymphoid tissue with or without germinal centers representing stages of TLS development (1, 32, 36-38). The total number of TLS detected per case was normalized to the total amount of biopsied renal cortex (mm^2) per case (34, 48).

Protein measurement

Urine and plasma samples were collected within a 2-hour window from time of laboratory arrival and aliquots were stored at -80ºC. Customized Luminex multiplex bead array assay (ProcartaPlex**,** ThermoFisher Scientific, Vienna, Austria) was used to determine the concentration of CCL2 (MCP1), CCL3 (macrophage inflammatory protein 1-alpha (MIP-1-alpha)), CCL4, CCL5 (RANTES), CCL8 (monocyte chemoattractant protein 2 (MCP2)), CCL18, CCL19, CCL21, CXCL9 (monokine induced by gamma interferon (MIG)), CXCL10, CXCL11 and CXCL13 in plasma and urine according to the manufacturer's protocol. Luminex MAGPIX multiplexing system was used to acquire data and xPONENT software (version 4.2) was used to analyze the data. All standards and samples were analyzed in duplicate. Urine specimens were normalized to urine creatinine measured using QuantiChrom™ Creatine Assay Kit - DICT-500 (BioAssay Systems, Hayward, CA).

RNA isolation and gene expression profiling

Total RNA was extracted and purified using the RNeasy Mini Kit (Qiagen GmbH, Hilden, Germany) according to manufacture instructions. Quantity and quality of RNA was assayed using Qubit RNA HS Assay Kit (ThermoFisher Scientific). RNA profiling was performed on 100 ng of RNA extracted from FFPE human kidney samples for the expression of 770 immune oncology-related genes and

housekeeping genes using the NanoString nCounter Human V.1.1 PanCancer Immune Profiling Panel (NanoString Technologies Inc, Seattle, WA). Raw data were normalized using the nSolver™ Analysis Software (Version 4.0) with the Advanced Analysis 2.0 plugin. Counts for target genes were normalized to internal synthetic positive controls and housekeeping genes. Data from the NanoString gene expression profiles have been submitted to the European Genome-phenome Archive (EGA) under accession no. EGAS00001006781.

Statistics

Expression profiling of RNA samples was evaluated by log2 normalized count data. Log2 normalized counts were used for individual gene analyses, scores for immune signatures were calculated by the geometric mean of signature genes. Urine chemokine to urine creatinine ratios and plasma chemokine levels were transformed to log2 counts. For all specimens, differences in the means of log2 count data were evaluated using one-way ANOVA and Tukey's multiple comparisons test. Statistical significance was considered at *$P<0.05$ and **$P<0.01$. For the volcano plots, ROSALIND cloud platform for nCounter data using Benjamini-Hochberg method was applied to calculate adjusted P-values with FDR threshold of 0.01 or 0.05 as specified. Statistical analyses were performed with GraphPad Prism 5.0 (GraphPad Software, Inc., San Diego, CA) and R version 4.1.1. Spearman's rho method was used to correlate chemokine expression between tissue vs plasma and tissue vs urine with Spearman's test used to compute exact p-values. Wilcoxon tests were used to determine p-values for the AUC (H0: AUC=0.5).

Study Approval

This study was approved by the MD Anderson Cancer Center Institutional Review Board in accordance with the Declaration of Helsinki under approval number PA19-0084.

AUTHOR CONTRIBUTIONS

Study was conceived and designed by C.Y. and J.S.L. Data acquisition was performed by S.S., A.T., Y.D., and J.S.L. S.S, J.P.L. and J.S.L. performed data analysis. A.T. performed the histological examination, provided images and description of the biopsied kidney specimens. S.S., J.P.L., A.T., C.Y., and J.P.L. contributed in writing the manuscript. The manuscript was prepared by S.S., C.Y. and J.S.L. All authors reviewed the manuscript at all stages. All the authors contributed to the quality control data, analysis, interpretation of data and writing and final proof of paper. All authors read and approved the final manuscript.

ACKNOWLEDGEMENTS

J.P.L. is partially supported by the National Cancer Institute and the National Center for Advancing Translational Sciences of the NIH P30CA016672 and CCTS UL1TR003167. C.Y. is Member of Parker Institute of Cancer Immunotherapy. J.S.L. is supported by the NIH/NIDDK (K08 DK119466). This research is also supported by the Division of Internal Medicine Immuno-Oncology Toxicity Award Program of the University of Texas MD Anderson Cancer Center (PI: J.S.L.) and the University Cancer Foundation via the Institutional Research Grant program at the University of Texas MD Anderson Cancer Center (PI: J.S.L.). The University of Texas MD Anderson Cancer Center is supported in part by the National Institutes of Health through Cancer Center Support Grant P30CA016672.

We thank the patients and their families for providing permission to report adverse events and for their participation and contribution to research. We are also grateful to Dr. Jerid Robinson from NanoString Technologies for his assistance with data support.

REFERENCES

1. Sautes-Fridman C, Petitprez F, Calderaro J, and Fridman WH. Tertiary lymphoid structures in the era of cancer immunotherapy. *Nat Rev Cancer.* 2019;19(6):307-25.
2. Pipi E, Nayar S, Gardner DH, Colafrancesco S, Smith C, and Barone F. Tertiary Lymphoid Structures: Autoimmunity Goes Local. *Front Immunol.* 2018;9:1952.
3. Vanhersecke L, Brunet M, Guégan J-P, Rey C, Bougouin A, Cousin S, et al. Mature tertiary lymphoid structures predict immune checkpoint inhibitor efficacy in solid tumors independently of PD-L1 expression. *Nature Cancer.* 2021;2(8):794-802.
4. Wang Y, Zhou S, Yang F, Qi X, Wang X, Guan X, et al. Treatment-Related Adverse Events of PD-1 and PD-L1 Inhibitors in Clinical Trials: A Systematic Review and Meta-analysis. *JAMA Oncol.* 2019;5(7):1008-19.
5. Bertrand A, Kostine M, Barnetche T, Truchetet ME, and Schaeverbeke T. Immune related adverse events associated with anti-CTLA-4 antibodies: systematic review and meta-analysis. *BMC Med.* 2015;13:211.
6. Cortazar FB, Marrone KA, Troxell ML, Ralto KM, Hoenig MP, Brahmer JR, et al. Clinicopathological features of acute kidney injury associated with immune checkpoint inhibitors. *Kidney Int.* 2016;90(3):638-47.
7. Meraz-Munoz A, Amir E, Ng P, Avila-Casado C, Ragobar C, Chan C, et al. Acute kidney injury associated with immune checkpoint inhibitor therapy: incidence, risk factors and outcomes. *J Immunother Cancer.* 2020;8(1).
8. Seethapathy H, Zhao S, Chute DF, Zubiri L, Oppong Y, Strohbehn I, et al. The Incidence, Causes, and Risk Factors of Acute Kidney Injury in Patients Receiving Immune Checkpoint Inhibitors. *Clin J Am Soc Nephrol.* 2019;14(12):1692-700.
9. Halimi JM, Gatault P, Longuet H, Barbet C, Bisson A, Sautenet B, et al. Major Bleeding and Risk of Death after Percutaneous Native Kidney Biopsies: A French Nationwide Cohort Study. *Clin J Am Soc Nephrol.* 2020;15(11):1587-94.

10. Baker ML, Yamamoto Y, Perazella MA, Dizman N, Shirali AC, Hafez N, et al. Mortality after acute kidney injury and acute interstitial nephritis in patients prescribed immune checkpoint inhibitor therapy. *Journal for ImmunoTherapy of Cancer.* 2022;10(3):e004421.
11. Atwell TD, Spanbauer JC, McMenomy BP, Stockland AH, Hesley GK, Schleck CD, et al. The Timing and Presentation of Major Hemorrhage After 18,947 Image-Guided Percutaneous Biopsies. *AJR Am J Roentgenol.* 2015;205(1):190-5.
12. Kang E, Park M, Park PG, Park N, Jung Y, Kang U, et al. Acute kidney injury predicts all-cause mortality in patients with cancer. *Cancer Med.* 2019;8(6):2740-50.
13. Poggio ED, McClelland RL, Blank KN, Hansen S, Bansal S, Bomback AS, et al. Systematic Review and Meta-Analysis of Native Kidney Biopsy Complications. *Clin J Am Soc Nephrol.* 2020;15(11):1595-602.
14. Cortazar FB, Kibbelaar ZA, Glezerman IG, Abudayyeh A, Mamlouk O, Motwani SS, et al. Clinical Features and Outcomes of Immune Checkpoint Inhibitor-Associated AKI: A Multicenter Study. *J Am Soc Nephrol.* 2020;31(2):435-46.
15. Kellum JA, and Lameire N. Diagnosis, evaluation, and management of acute kidney injury: a KDIGO summary (Part 1). *Crit Care.* 2013;17(1):204.
16. Roufosse C, Simmonds N, Clahsen-van Groningen M, Haas M, Henriksen KJ, Horsfield C, et al. A 2018 Reference Guide to the Banff Classification of Renal Allograft Pathology. *Transplantation.* 2018;102(11):1795-814.
17. Danaher P, Warren S, Dennis L, D'Amico L, White A, Disis ML, et al. Gene expression markers of Tumor Infiltrating Leukocytes. *J Immunother Cancer.* 2017;5:18.
18. Sharpe C, Davis J, Mason K, Tam C, Ritchie D, and Koldej R. Comparison of gene expression and flow cytometry for immune profiling in chronic lymphocytic leukaemia. *J Immunol Methods.* 2018;463:97-104.
19. Kim ST, Chu Y, Misoi M, Suarez-Almazor ME, Tayar JH, Lu H, et al. Distinct molecular and immune hallmarks of inflammatory arthritis induced by immune checkpoint inhibitors for cancer therapy. *Nature Communications.* 2022;13(1):1970.

20. Hone Lopez S, Kats-Ugurlu G, Renken RJ, Buikema HJ, de Groot MR, Visschedijk MC, et al. Immune checkpoint inhibitor treatment induces colitis with heavy infiltration of CD8 + T cells and an infiltration pattern that resembles ulcerative colitis. *Virchows Arch.* 2021;479(6):1119-29.

21. Westdorp H, Sweep MWD, Gorris MAJ, Hoentjen F, Boers-Sonderen MJ, van der Post RS, et al. Mechanisms of Immune Checkpoint Inhibitor-Mediated Colitis. *Front Immunol.* 2021;12:768957.

22. Sasson SC, Slevin SM, Cheung VTF, Nassiri I, Olsson-Brown A, Fryer E, et al. Interferon-Gamma–Producing CD8+ Tissue Resident Memory T Cells Are a Targetable Hallmark of Immune Checkpoint Inhibitor–Colitis. *Gastroenterology.* 2021;161(4):1229-44.e9.

23. Cappelli LC, Gutierrez AK, Baer AN, Albayda J, Manno RL, Haque U, et al. Inflammatory arthritis and sicca syndrome induced by nivolumab and ipilimumab. *Ann Rheum Dis.* 2017;76(1):43-50.

24. Johnson DH, Zobniw CM, Trinh VA, Ma J, Bassett RL, Jr., Abdel-Wahab N, et al. Infliximab associated with faster symptom resolution compared with corticosteroids alone for the management of immune-related enterocolitis. *J Immunother Cancer.* 2018;6(1):103.

25. Lin JS, Mamlouk O, Selamet U, Tchakarov A, Glass WF, Sheth RA, et al. Infliximab for the treatment of patients with checkpoint inhibitor-associated acute tubular interstitial nephritis. *Oncoimmunology.* 2021;10(1):1877415.

26. Tang H, Zhu M, Qiao J, and Fu YX. Lymphotoxin signalling in tertiary lymphoid structures and immunotherapy. *Cell Mol Immunol.* 2017;14(10):809-18.

27. Coppola D, Nebozhyn M, Khalil F, Dai H, Yeatman T, Loboda A, et al. Unique Ectopic Lymph Node-Like Structures Present in Human Primary Colorectal Carcinoma Are Identified by Immune Gene Array Profiling. *The American Journal of Pathology.* 2011;179(1):37-45.

28. Messina JL, Fenstermacher DA, Eschrich S, Qu X, Berglund AE, Lloyd MC, et al. 12-Chemokine gene signature identifies lymph node-like structures in melanoma: potential for patient selection for immunotherapy? *Sci Rep.* 2012;2:765.

29. Prabhakaran S, Rizk VT, Ma Z, Cheng C-H, Berglund AE, Coppola D, et al. Evaluation of invasive breast cancer samples using a 12-chemokine gene expression score: correlation with clinical outcomes. *Breast Cancer Research.* 2017;19(1):71.

30. Luther SA, Lopez T, Bai W, Hanahan D, and Cyster JG. BLC expression in pancreatic islets causes B cell recruitment and lymphotoxin-dependent lymphoid neogenesis. *Immunity.* 2000;12(5):471-81.

31. Mebius RE. Organogenesis of lymphoid tissues. *Nat Rev Immunol.* 2003;3(4):292-303.

32. Hill DG, Yu L, Gao H, Balic JJ, West A, Oshima H, et al. Hyperactive gp130/STAT3-driven gastric tumourigenesis promotes submucosal tertiary lymphoid structure development. *Int J Cancer.* 2018;143(1):167-78.

33. Cabrita R, Lauss M, Sanna A, Donia M, Skaarup Larsen M, Mitra S, et al. Tertiary lymphoid structures improve immunotherapy and survival in melanoma. *Nature.* 2020;577(7791):561-5.

34. Gao J, Navai N, Alhalabi O, Siefker-Radtke A, Campbell MT, Tidwell RS, et al. Neoadjuvant PD-L1 plus CTLA-4 blockade in patients with cisplatin-ineligible operable high-risk urothelial carcinoma. *Nat Med.* 2020;26(12):1845-51.

35. Gu-Trantien C, Loi S, Garaud S, Equeter C, Libin M, de Wind A, et al. CD4(+) follicular helper T cell infiltration predicts breast cancer survival. *J Clin Invest.* 2013;123(7):2873-92.

36. Siliņa K, Soltermann A, Attar FM, Casanova R, Uckeley ZM, Thut H, et al. Germinal Centers Determine the Prognostic Relevance of Tertiary Lymphoid Structures and Are Impaired by Corticosteroids in Lung Squamous Cell Carcinoma. *Cancer Res.* 2018;78(5):1308-20.

37. Schumacher TN, and Thommen DS. Tertiary lymphoid structures in cancer. *Science.* 2022;375(6576):eabf9419.

38. Cipponi A, Mercier M, Seremet T, Baurain JF, Théate I, van den Oord J, et al. Neogenesis of lymphoid structures and antibody responses occur in human melanoma metastases. *Cancer Res.* 2012;72(16):3997-4007.

39. Nera K-P, Kyläniemi MK, and Lassila O. Regulation of B Cell to Plasma Cell Transition within the Follicular B Cell Response. *Scandinavian Journal of Immunology.* 2015;82(3):225-34.

40. Thaunat O, Patey N, Caligiuri G, Gautreau C, Mamani-Matsuda M, Mekki Y, et al. Chronic Rejection Triggers the Development of an Aggressive Intragraft Immune Response through Recapitulation of Lymphoid Organogenesis. *The Journal of Immunology.* 2010;185(1):717-28.

41. Praga M, and Gonzalez E. Acute interstitial nephritis. *Kidney Int.* 2010;77(11):956-61.

42. Shirali AC, Perazella MA, and Gettinger S. Association of Acute Interstitial Nephritis With Programmed Cell Death 1 Inhibitor Therapy in Lung Cancer Patients. *Am J Kidney Dis.* 2016;68(2):287-91.

43. Gupta S, Cortazar FB, Riella LV, and Leaf DE. Immune Checkpoint Inhibitor Nephrotoxicity: Update 2020. *Kidney360.* 2020;1(2):130-40.

44. Soukou S, Huber S, and Krebs CF. T cell plasticity in renal autoimmune disease. *Cell and Tissue Research.* 2021;385(2):323-33.

45. Paust HJ, Turner JE, Riedel JH, Disteldorf E, Peters A, Schmidt T, et al. Chemokines play a critical role in the cross-regulation of Th1 and Th17 immune responses in murine crescentic glomerulonephritis. *Kidney Int.* 2012;82(1):72-83.

46. Tokunaga R, Zhang W, Naseem M, Puccini A, Berger MD, Soni S, et al. CXCL9, CXCL10, CXCL11/CXCR3 axis for immune activation – A target for novel cancer therapy. *Cancer Treatment Reviews.* 2018;63:40-7.

47. Mehta NN, Teague HL, Swindell WR, Baumer Y, Ward NL, Xing X, et al. IFN-γ and TNF-α synergism may provide a link between psoriasis and inflammatory atherogenesis. *Scientific Reports.* 2017;7(1):13831.

48. Helmink BA, Reddy SM, Gao J, Zhang S, Basar R, Thakur R, et al. B cells and tertiary lymphoid structures promote immunotherapy response. *Nature.* 2020;577(7791):549-55.

49. Cabrita R, Lauss M, Sanna A, Donia M, Skaarup Larsen M, Mitra S, et al. Author Correction: Tertiary lymphoid structures improve immunotherapy and survival in melanoma. *Nature.* 2020;580(7801):E1.

50. Germain C, Gnjatic S, Tamzalit F, Knockaert S, Remark R, Goc J, et al. Presence of B cells in tertiary lymphoid structures is associated with a protective immunity in patients with lung cancer. *Am J Respir Crit Care Med.* 2014;189(7):832-44.

51. Di Caro G, Bergomas F, Grizzi F, Doni A, Bianchi P, Malesci A, et al. Occurrence of tertiary lymphoid tissue is associated with T-cell infiltration and predicts better prognosis in early-stage colorectal cancers. *Clin Cancer Res.* 2014;20(8):2147-58.

52. Khan S, Khan SA, Luo X, Fattah FJ, Saltarski J, Gloria-McCutchen Y, et al. Immune dysregulation in cancer patients developing immune-related adverse events. *Br J Cancer.* 2019;120(1):63-8.

53. Tokunaga R, Zhang W, Naseem M, Puccini A, Berger MD, Soni S, et al. CXCL9, CXCL10, CXCL11/CXCR3 axis for immune activation - A target for novel cancer therapy. *Cancer Treat Rev.* 2018;63:40-7.

54. Dorraji SE, Kanapathippillai P, Hovd A-MK, Stenersrød MR, Horvei KD, Ursvik A, et al. Kidney Tertiary Lymphoid Structures in Lupus Nephritis Develop into Large Interconnected Networks and Resemble Lymph Nodes in Gene Signature. *The American Journal of Pathology.* 2020;190(11):2203-25.

55. Chen W, Li W, Zhang Z, Tang X, Wu S, Yao G, et al. Lipocalin-2 Exacerbates Lupus Nephritis by Promoting Th1 Cell Differentiation. *Journal of the American Society of Nephrology.* 2020;31(10):2263-77.

56. Lee YH, Sato Y, Saito M, Fukuma S, Saito M, Yamamoto S, et al. Advanced Tertiary Lymphoid Tissues in Protocol Biopsies are Associated with Progressive Graft Dysfunction in Kidney Transplant Recipients. *Journal of the American Society of Nephrology.* 2022;33(1):186-200.

57. Gupta S, Short SAP, Sise ME, Prosek JM, Madhavan SM, Soler MJ, et al. Acute kidney injury in patients treated with immune checkpoint inhibitors. *J Immunother Cancer.* 2021;9(10).

58. Croft M. The role of TNF superfamily members in T-cell function and diseases. *Nat Rev Immunol.* 2009;9(4):271-85.

59. Figgett WA, Vincent FB, Saulep-Easton D, and Mackay F. Roles of ligands from the TNF superfamily in B cell development, function, and regulation. *Semin Immunol.* 2014;26(3):191-202.

60. Moledina DG, Wilson FP, Pober JS, Perazella MA, Singh N, Luciano RL, et al. Urine TNF-alpha and IL-9 for clinical diagnosis of acute interstitial nephritis. *JCI Insight.* 2019;4(10).

61. Wong YNS, Joshi K, Khetrapal P, Ismail M, Reading JL, Sunderland MW, et al. Urine-derived lymphocytes as a non-invasive measure of the bladder tumor immune microenvironment. *Journal of Experimental Medicine.* 2018;215(11):2748-59.

62. Kopetschke K, Klocke J, Griessbach AS, Humrich JY, Biesen R, Dragun D, et al. The cellular signature of urinary immune cells in Lupus nephritis: new insights into potential biomarkers. *Arthritis Res Ther.* 2015;17:94.

63. Sakatsume M, Xie Y, Ueno M, Obayashi H, Goto S, Narita I, et al. Human glomerulonephritis accompanied by active cellular infiltrates shows effector T cells in urine. *J Am Soc Nephrol.* 2001;12(12):2636-44.

64. Goerlich N, Brand HA, Langhans V, Tesch S, Schachtner T, Koch B, et al. Kidney transplant monitoring by urinary flow cytometry: Biomarker combination of T cells, renal tubular epithelial cells, and podocalyxin-positive cells detects rejection. *Sci Rep.* 2020;10(1):796.

Figures and Figure Legends

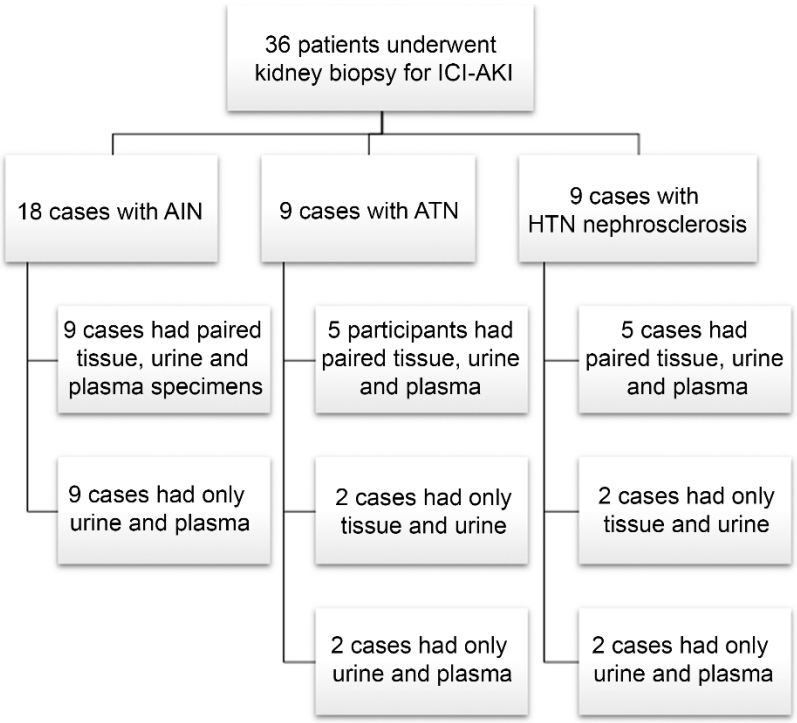

Figure 1. Flow diagram of kidney injury subgroups and samples analyzed.

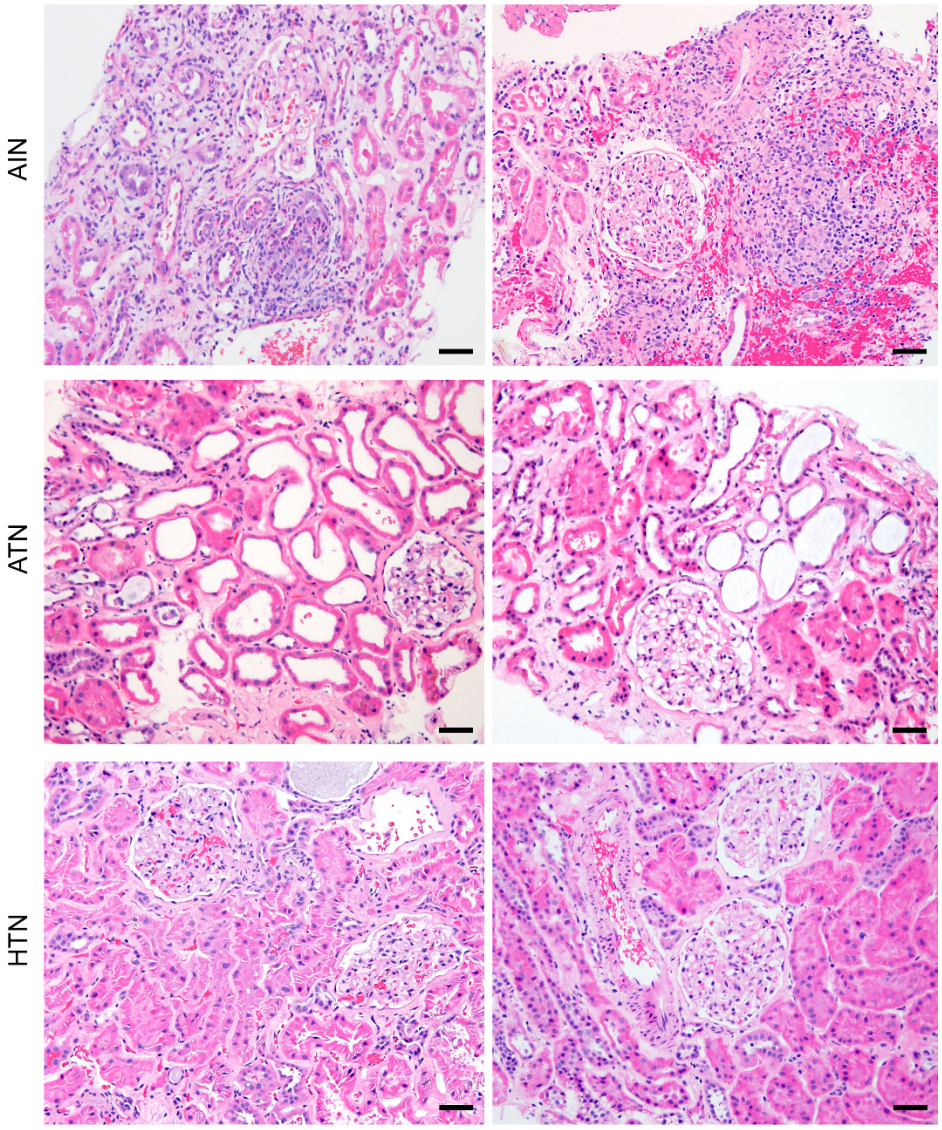

Figure 2. Representative hematoxylin and eosin (H&E) staining of kidney biopsy sections from two different patients in each subgroup. Scale bar = 50 μm.

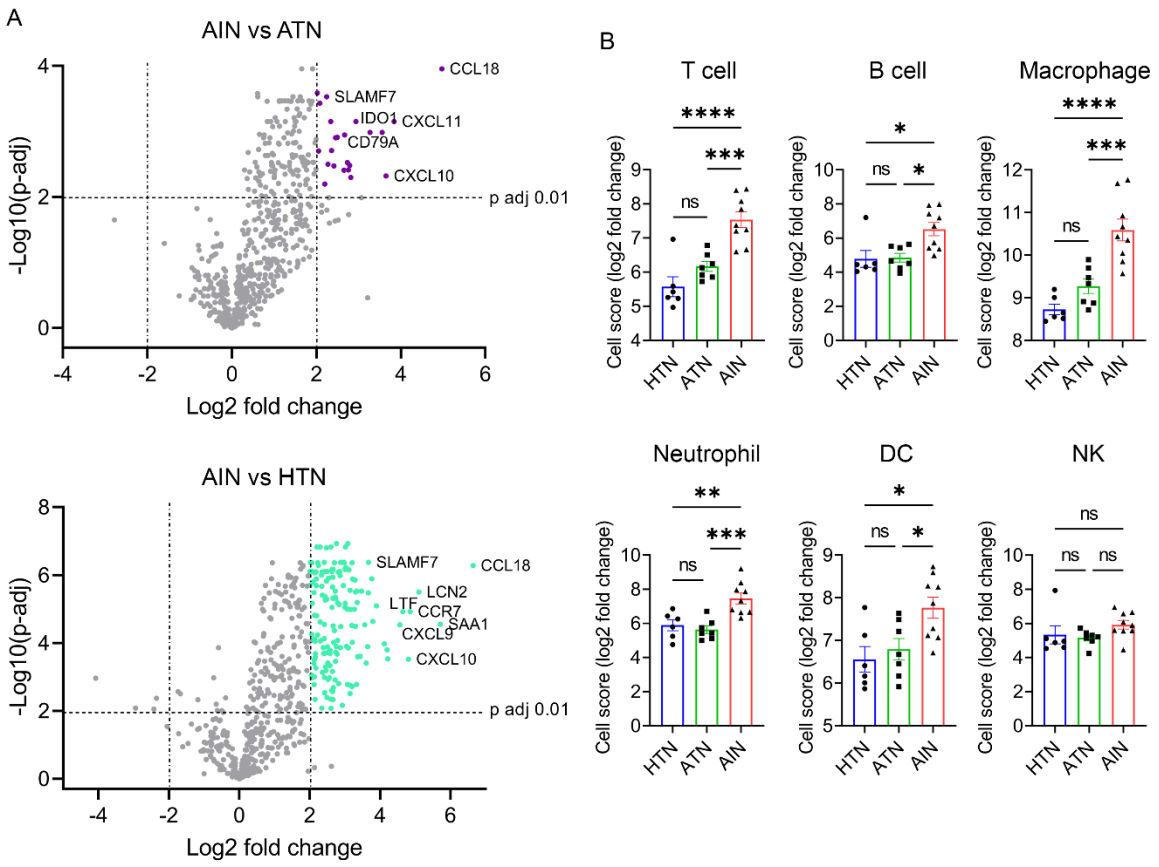

Figure 3. Identification of differentially expressed genes and relative abundance of immune cells in kidney injury. A. Volcano plot for differentially expressed genes between AIN vs ATN and AIN vs HTN. Each dot represents a single gene, x-axis shows log2 fold change and y-axis shows log 10 change in statistical significance (p-adj value). Genes upregulated (log 2-fold or 4-fold linear) in AIN group are highlighted. Purple dots represent genes upregulated in AIN group compared to ATN group and green dots represent genes upregulated in AIN group compared to HTN group. **B.** Expression of specific gene signature was used to determine immune cell score for infiltrating T cells, B cells, macrophages, neutrophils, dendritic cells and NK cells in different groups. Data represents cell score (log2 fold change) geometric mean ± SEM for different groups. P value represents statistical analysis by Tukey's multiple comparison test, *p<0.05, **p<0.01, ***p<0.0005, **** p<0.0001, (adj p value).

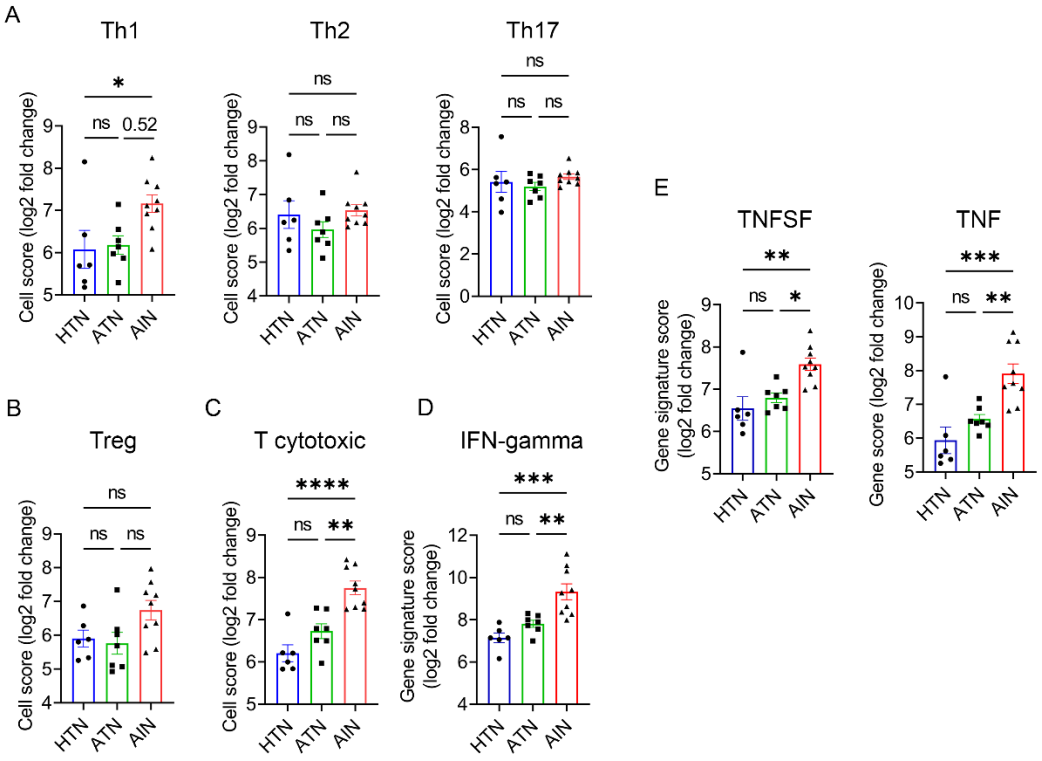

Figure 4. Identification, abundance and function of the different T cell subsets in kidney biopsies of patients with ICI-AIN, ATN and HTN. Specific gene signatures were used to determine cell score. **A.** Abundance of T helper subsets, Th1, Th2 and Th17 **B.** Treg and **C.** cytotoxic T cells score was determined and compared between three groups. Data represents cell score (log2 fold change) geometric mean ± SEM for different groups. The p values were determined using Tukey's multiple comparisons test *p<0.05, **p<0.01, ***p<0.0005, **** p<0.0001 (adj p value). Gene signature score for T cell effector function mediated by **D.** IFN-γ (*IFNG, STAT1, CCR5, CXCL9, CXCL10, CXCL11, IDO1, PRF1, GZMA, HLA-DRA*) and **E.** TNF superfamily (TNFSF) and TNF expression was calculated and compared for the three groups. Data represents the gene signature score (log2 fold change) ± SEM for different groups and Tukey's multiple comparison test was used for statistical analysis, *p<0.05, **p<0.01, ***p<0.0005, (adj p value).

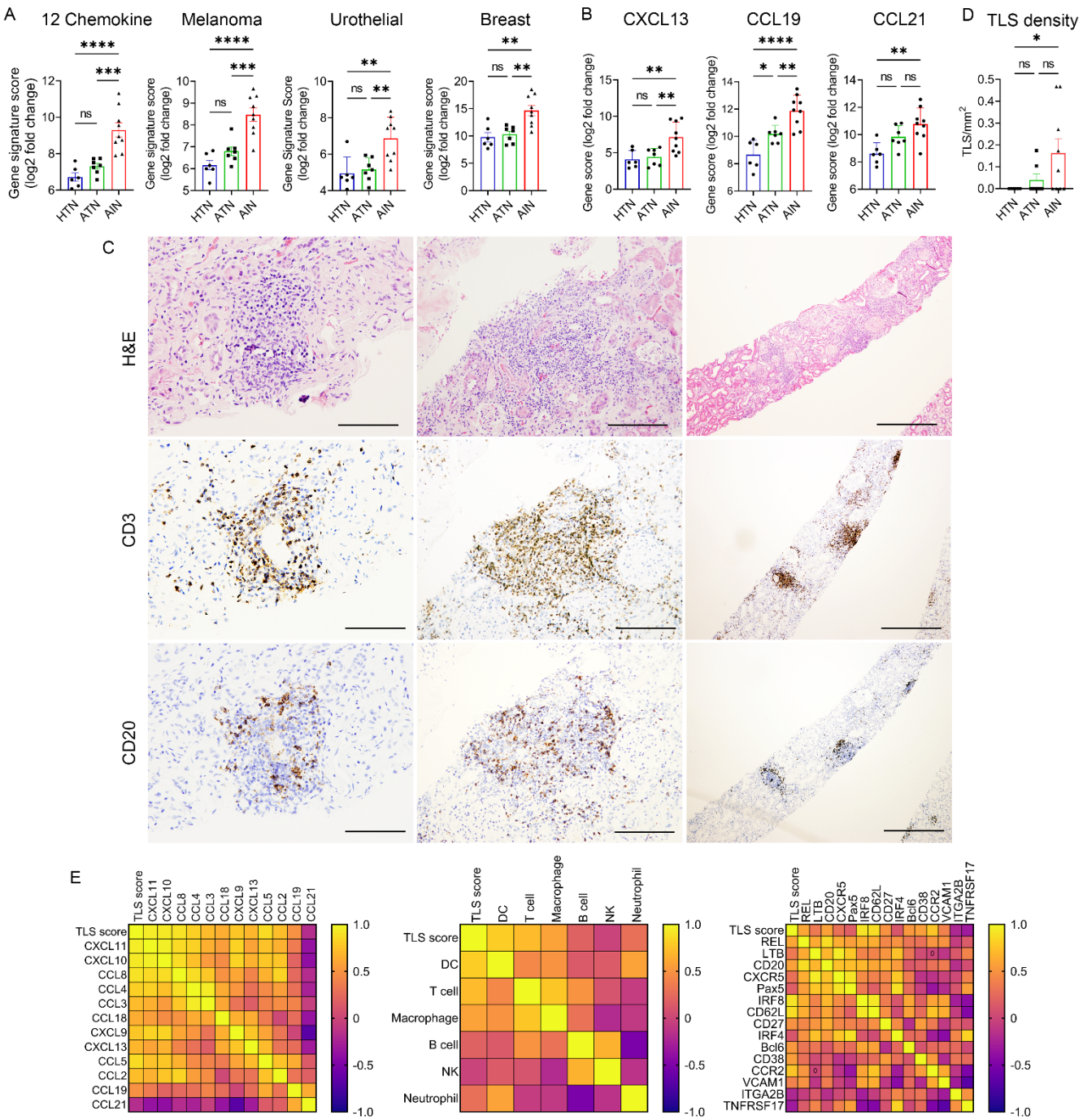

Figure 5. Transcriptional and histopathological analysis of TLS in kidney biopsy of AIN, ATN and HTN. A. Gene expression of 12 chemokines along with genes associated with melanoma, urothelial cancer and breast cancer TLS signatures was used to determine the transcription gene score **B.** Gene scores for *CXCL13, CCL19, CCL21* compared among AIN, ATN and HTN groups. Data represents geometric mean (log 2-fold change) ± SEM and p value were determined using Tukey's multiple comparisons test, *p<0.05, **p<0.01, ***p<0.0005, ****p<0.0001 (adj p value). **C.** Representative H&E staining of kidney biopsy showing organized lymphocyte aggregates with $CD20^+$ B cells adjacent to a $CD3^+$ T cell zone (scale bar 100um). **D.** Density of TLS per mm^2 of biopsied renal cortex per case. Data are presented as mean ± SEM for different groups and p value was determined using Tukey's multiple comparisons test, *p<0.05. **E.** Heatmap of supervised clustering of differentially expressed genes for 12 chemokines, immune cells types and B cell activation and differentiation in AIN group is shown.

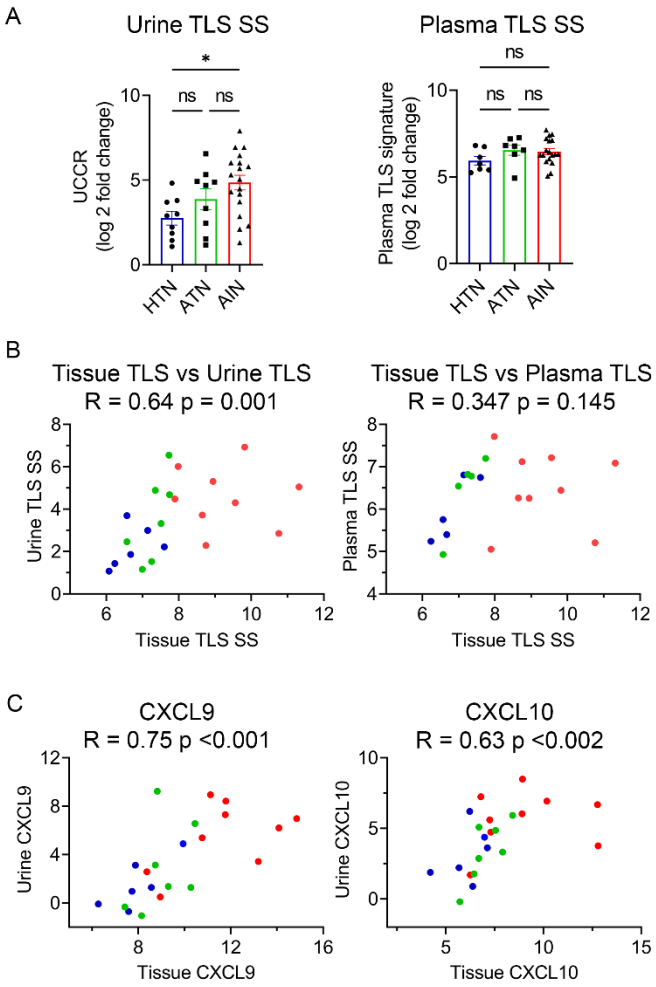

Figure 6. TLS detection based on chemokines present in urine and plasma of patients with ICI-AIN, ATN or HTN. Chemokines associated with TLS gene signature were measured in urine and plasma using Luminex based multiplex chemokine assay. **A.** Urine chemokine levels were adjusted for urine creatinine levels and the urine chemokine to urine creatinine ratio (UCCR) was log 2 transformed. Urine TLS score was determined as the arthrimetic mean of the 12 UCCR. Plasma TLS scores were assessed for each of the 12 chemokines. Data represents protein concentration (log2 fold change) arthrimetic mean ± SEM for different groups. The p values were determined using Tukey's multiple comparisons test, *p<0.05 (adj p value). **B.** Correlation between tissue TLS signature score and urine TLS signature score and tissue TLS signature score and plasma TLS signature score. **C.** Correlation between gene expression in tissue and cytokine in urine for CXCL9 and CXCL10. R represents Spearman's rho, a non-parametric measure of correlation. Spearman's test used to assess whether correlations were non-zero (H0: rho=0). Abbreviation: SS, signature score.

Table 1. Demographic and Clinical characteristics of the cases

Characteristic	AIN, N = 18[1]	ATN, N = 9[1]	HTN, N = 9[1]	p-value[2]
Sex				0.6
F	6 (33%)	5 (56%)	4 (44%)	
M	12 (67%)	4 (44%)	5 (56%)	
Age	67 (56, 73)	60 (54, 63)	68 (55, 73)	0.4
Malignancy				>0.9
Bladder	1 (5.6%)	0 (0%)	1 (11%)	
Breast	1 (5.6%)	0 (0%)	1 (11%)	
Colon	1 (5.6%)	0 (0%)	0 (0%)	
Lung	2 (11%)	3 (33%)	1 (11%)	
Melanoma	6 (33%)	2 (22%)	2 (22%)	
RCC	3 (17%)	1 (11%)	1 (11%)	
Sq cell oral cavity	1 (5.6%)	1 (11%)	2 (22%)	
Thyroid	2 (11%)	0 (0%)	0 (0%)	
Other/Unknown	1 (5.6%)	2 (22%)	1 (11%)	
Time to AKI (days)	146 (52, 264)	67 (48, 124)	196 (137, 275)	0.084
ICI				0.9
PD1	11 (61%)	7 (78%)	5 (56%)	
PD-L1	1 (5.6%)	0 (0%)	1 (11%)	
Combo	6 (33%)	2 (22%)	3 (33%)	
KDIGO AKI Stage				0.016
1	4 (22%)	3 (33%)	8 (89%)	
2	4 (22%)	3 (33%)	0 (0%)	
3	10 (56%)	3 (33%)	1 (11%)	
UA Active	11 (61%)	4 (44%)	3 (33%)	0.4
Baseline Creatinine	1.00 (0.91, 1.17)	0.90 (0.83, 1.19)	1.33 (1.20, 1.50)	0.022
Peak Creatinine	3.45 (2.26, 4.08)	2.15 (1.73, 4.39)	1.90 (1.49, 2.00)	0.020
Creatinine Ratio	3.47 (2.03, 5.08)	2.59 (1.60, 5.49)	1.28 (1.27, 1.75)	0.002
Inflammation %				<0.001
0	0 (0%)	0 (0%)	2 (22%)	
<25%	1 (5.6%)	8 (89%)	7 (78%)	
25-50%	5 (28%)	0 (0%)	0 (0%)	
>50%	12 (67%)	1 (11%)	0 (0%)	
IFTA	10 (0, 20)	10 (0, 10)	10 (5, 20)	0.7
Unknown	1	0	0	
GS	14 (8, 22)	6 (2, 15)	18 (2, 27)	0.5
Treated w/steroids	17 (94%)	1 (11%)	1 (11%)	<0.001
Renal Recovery				0.4
CR	7 (39%)	2 (22%)	5 (56%)	
PR	8 (44%)	7 (78%)	3 (33%)	
NR	3 (17%)	0 (0%)	1 (11%)	
Restarted ICI Therapy	2 (11%)	6 (67%)	9 (100%)	<0.001

[1]n (%); Median (IQR)

[2]Fisher's exact test; Kruskal-Wallis rank sum test

Abbreviations: AIN, acute interstitial nephritis; ATN, acute tubular necrosis; HTN, hypertensive nephrosclerosis; ICI, immune checkpoint inhibitor; F, female; M, male; RCC, renal cell carcinoma; Sq cell, squamous cell carcinoma; PD1, programmed cell death protein 1; PD-L1, programmed death-ligand 1; KDIGO, Kidney Disease: Improving Global Outcomes; AKI, acute kidney injury; UA, urinalysis, IFTA, interstitial fibrosis tubular atrophy; GS, glomerulosclerosis; CR, complete recovery; PR, partial recovery; NR, no recovery

Table 2. Top 10 differentially expressed genes between AIN vs ATN

Gene Symbol	Log2 Fold Change	p-Value	p-Adj
CCL18	4.974	5.30E-07	1.11E-04
CXCL11	3.840	4.11E-05	7.06E-04
CXCL10	3.648	9.82E-04	4.79E-03
CXCL9	3.556	7.88E-05	1.03E-03
S100A8	3.270	7.74E-05	1.03E-03
IDO1	2.939	4.59E-05	7.06E-04
CXCL8	2.817	1.05E-03	5.04E-03
TREM1	2.792	5.23E-04	3.32E-03
CXCL7	2.758	7.00E-04	3.89E-03
SLAMF7	2.736	4.48E-04	2.97E-03

Benjamini-Hochberg method was applied to calculate adjusted P-values with FDR threshold of 0.01.

Table 3. Top 10 differentially expressed genes between AIN vs HTN.

Gene Symbol	Log2 fold Change	p-Value	p-Adj
CCL18	6.647	1.98E-08	5.22E-07
SAA1	5.717	6.27E-06	2.80E-05
LCN2	5.107	4.14E-07	3.17E-06
CCR7	4.860	2.46E-06	1.20E-05
CXCL10	4.810	9.99E-05	3.00E-04
LTF	4.649	2.44E-06	1.20E-05
CXCL9	4.566	6.67E-06	2.92E-05
CXCL6	4.222	9.75E-05	2.95E-04
CCL13	4.204	4.82E-05	1.60E-04
C3	4.127	2.95E-05	1.06E-04

Benjamini-Hochberg method was applied to calculate adjusted P-values with FDR threshold of 0.01.

Table 4. Top 5 TNF superfamily (TNFSF) genes upregulated in AIN vs ATN

Gene symbol (alias)	Log2 fold Change	p-Value	p-Adj
TNFRSF4 (*OX40*)	2.341	4.43E-05	7.06E-04
TNFRSF13C (*BAFFR*)	2.250	4.56E-3	1.59E-02
LTB	1.828	4.22E-04	2.95E-03
TNFSF14 (*LIGHT*)	1.798	9.89E-03	2.78E-02
TNFRSF17 (*BCMA*)	1.672	1.90E-04	1.73E-03

Benjamini-Hochberg method was applied to calculate adjusted P-values with FDR threshold of 0.01.

Table 5. Top 5 TNF superfamily (TNFSF) genes upregulated in AIN vs HTN

Gene symbol (alias)	Log2 fold Change	p-Value	p-Adj
TNFSF14 (*LIGHT*)	3.769	1.07E-07	1.28E-06
TNFRSF4 (*OX40*)	3.667	4.54E-07	3.33E-06
LTB	3.209	1.41E-08	4.35E-07
TNFRSF18	2.664	7.40E-07	4.91E-06
TNFRSF13C (*BAFFR*)	2.599	2.27E-03	4.55E-03

Benjamini-Hochberg method was applied to calculate adjusted P-values with FDR threshold of 0.01.

Table 6. Predictive AUC for ICI-AIN

Method	AUC	p-Value
Tissue TLS Signature Score	1.000	<0.001
TLS Density	0.841	<0.001
Urine TLS Signature Score	0.735	0.016
Plasma TLS Signature Score	0.556	0.613

AUC=1 indicates that the given marker can perfectly separate AIN from non-AIN and AUC ≤0.5 indicates the marker has no ability to separate the two groups. Wilcoxon tests were used to determine p-values for the AUC (H0: AUC=0.5), with a low p-value indicating that it is unlikely that the true AUC is 0.5 (i.e. unlikely the marker has no ability to distinguish AIN from non-AIN).

Table 7. TLS signature vs individual urine marker

Urine Marker	rho	p-value
CXCL9	0.658	<0.001
CCL19	0.642	0.001
CCL2	0.599	0.003
CCL3	0.597	0.004
CXCL13	0.573	0.005
CCL4	0.560	0.007
CXCL10	0.531	0.011
CCL21	0.445	0.038
CCL18	0.383	0.087
CXCL11	0.335	0.138
CCL5	0.278	0.210
CCL8	0.161	0.486

Spearman's test used to assess whether correlations were non-zero (H0: rho=0).

Table 8. Correlation tissue vs urine marker

	Tissue-Urine	
Marker	rho	p-value
CXCL9	0.75	<0.001
CXCL10	0.63	0.002
CCL19	0.56	0.007
CCL2	0.54	0.011
CCL4	0.50	0.018
CCL21	0.50	0.019
CCL18	0.45	0.040
CCL5	0.38	0.078
CCL3	0.32	0.160
CXCL13	0.21	0.337
CXCL11	0.14	0.537
CCL8	-0.10	0.678

Spearman's test used to assess whether correlations were non-zero (H0: rho=0).

Table 9. Marker ability to discriminate AIN vs non-AIN

	Tissue		Urine	
Marker	AUC	p-value	AUC	p-value
CXCL9	0.906	<0.001	0.781	0.003
CXCL10	0.829	0.009	0.802	0.001
CCL19	0.940	<0.001	0.682	0.064
CCL2	0.863	0.003	0.639	0.161
CCL4	0.803	0.017	0.611	0.269
CCL21	0.846	0.006	0.719	0.026
CCL18	0.983	<0.001	0.529	0.782
CCL5	0.966	<0.001	0.627	0.203
CCL3	0.838	0.007	0.703	0.041
CXCL13	0.863	0.003	0.731	0.017
CXCL11	0.880	0.002	0.665	0.109
CCL8	0.915	<0.001	0.618	0.245

AUC=1 indicates that the given marker can perfectly separate AIN from non-AIN and AUC ≤0.5 indicates the marker has no ability to separate the two groups. Wilcoxon tests were used to determine p-values for the AUC (H0: AUC=0.5), with a low p-value indicating that it is unlikely that the true AUC is 0.5 (i.e. unlikely the marker has no ability to distinguish AIN from non-AIN).